Applied Catalysis A, General 569 (2019) 1–7

Contents lists available at ScienceDirect

Applied Catalysis A, General

journal homepage: www.elsevier.com/locate/apcata

Investigation of ZSM-5 catalysts for dimethylether conversion using inelastic neutron scattering

Andrea Zachariou[a,b], Alexander Hawkins[a,b], David Lennon[a], Stewart F. Parker[b,c], Suwardiyanto[d], Santhosh K. Matam[b,e], C. Richard A. Catlow[b,e,f], Paul Collier[g], Ali Hameed[h], James McGregor[h], Russell F. Howe[i,*]

[a] School of Chemistry, Joseph Black Building, University of Glasgow, Glasgow, G12 8QQ, UK
[b] UK Catalysis Hub, Research Complex at Harwell, STFC Rutherford Appleton Laboratory, Chilton, Oxon, OX11 0FA, UK
[c] ISIS Facility, STFC Rutherford Appleton Laboratory, Chilton, Oxon, OX11 0QX, UK
[d] Department of Chemistry, University of Jember, Jember, Indonesia
[e] Department of Chemistry, University College London, 20 Gordon St., London, WC1 HOAJ, UK
[f] School of Chemistry, Cardiff University, Cardiff, CF10 1AT, UK
[g] Johnson Matthey Technology Centre, Blounts Court, Sonning Common, Reading RG4 9NH, UK
[h] Department of Chemical and Biological Engineering, University of Sheffield, Sheffield, S1 3JD, UK
[i] Department of Chemistry, University of Aberdeen, Aberdeen, AB24 3UE, UK

ARTICLE INFO

This paper is dedicated to Chuck Peden on the occasion of his 65th birthday.

Keywords:
ZSM-5
Inelastic neutron scattering
Dimethylether
Coke formation

ABSTRACT

We report the characterisation of zeolite ZSM-5 catalysts used in the conversion of dimethylether to hydrocarbons. Inelastic neutron scattering spectroscopy, supported by solid state NMR, shows that the more rapid deactivation occurring with dimethylether compared with methanol is associated with the formation of less methylated aromatic coke species and attributed to the lower levels of water present during dimethylether conversion. The ability of inelastic neutron scattering to probe a working catalyst with no sample preparation is demonstrated.

1. Introduction

Methanol to hydrocarbons (MTH), is a catalytic reaction which uses an acidic zeolite to convert methanol into light olefins (MTO) or gasoline range hydrocarbons (MTG). [1,2]. ZSM-5 is a commonly used catalyst for the reaction due to its shape selectivity and Brønsted acidity [3–6]. Even though the reaction has already been industrialised, the mechanism is still heavily debated. The most widely accepted mechanism is the 'Hydrocarbon Pool Mechanism', where the hydrocarbons formed within the catalyst act both as the activating and deactivating species [1,7–9]. The challenge in identifying the mechanism stems from the complex nature of the reaction. Changes in the nature of the catalyst such as the Si/Al ratio, or the reaction conditions can lead to changes in product distribution, feedstock conversion and catalyst deactivation [4,7,10–12].

There is an extensive literature on the MTH reaction [3,7–9,13,14]. In certain variations of the process utilising a fixed bed reactor, the feedstock is an equilibrated mixture of methanol, dimethylether (DME) and water [15,16]. Recent work has suggested that the mechanistic steps of methanol and of DME used as feedstock may not be the same. [12,15–17]. Kinetic studies have indicated that DME converts faster and at lower temperatures to olefins than methanol [12,18]. Deactivation studies have also shown that the catalyst deactivates at a faster rate with dimethylether [12,16]. The fast deactivation has been attributed to the lower water concentration and the faster kinetics of the reaction when DME is used [12].

The mechanism of the MTH reaction is elusive due to the constant changing nature of the hydrocarbon pool which makes it difficult to characterise fully. Different analytical techniques have been employed in the past in order to study the hydrocarbons retained within the zeolite. Conventional optical spectroscopies such as infrared and Raman as well as NMR have been used to characterise the hydrocarbon pool [7]. The importance of identifying the active hydrocarbons retained in the zeolite is undisputed and deactivated samples are of the same importance when it comes to an increased understanding of the MTH chemistry. Therefore, coke identification is just as significant and just as

* Corresponding author.
E-mail address: r.howe@abdn.ac.uk (R.F. Howe).

https://doi.org/10.1016/j.apcata.2018.10.010
Received 16 August 2018; Received in revised form 3 October 2018; Accepted 7 October 2018
Available online 09 October 2018

difficult as the active species characterisation. Temperature Programmed Oxidation (TPO) can provide information about the quantity of carbon present within a catalyst sample [7,19]. The Guisnet method is the only method to date that can identify the specific hydrocarbons present in the zeolite and quantify them [20]. It involves dissolving the zeolite in 40% HF and extracting the hydrocarbons retained within the zeolite pores [20]. The extracted hydrocarbons can then be analysed and quantified by GC–MS or any other suitable technique. However, the Guisnet method destroys the zeolite completely, which could sometimes be problematic.

Recently, inelastic neutron scattering (INS) has been used to study the ZSM-5 catalyst used in MTH reactions [8,21,22]. INS is a spectroscopic technique which offers a new perspective in the studying of catalytic reactions [23,24]. It can access the full vibrational spectrum of the hydrocarbon pool (0-4000 cm^{-1}) with no obstruction from the zeolite framework, as well as no restriction from the catalyst deactivation via coke deposition [8].

This work focuses on using a combination of INS, TPO and NMR in order to study the changes in the nature of the hydrocarbon pool when using DME as feedstock, ZSM-5 as the catalyst and following the reaction through to deactivation. We have previously undertaken a similar analysis on methanol reactions [8,21]. An industrial grade ZSM-5 catalyst was reacted at a constant temperature of 350 °C with varying DME feed rates and times-on-stream. The reaction was monitored by in-line mass spectrometric analysis of the gaseous products and off line GC–MS analysis of the liquid products. The combination of INS spectroscopy with the TPO and NMR analyses provides a platform to understand the retained hydrocarbons in the deactivated catalysts.

2. Experimental

2.1. Catalyst preparation and reaction testing

The catalyst used is a commercial ZSM-5 zeolite powder provided by Johnson Matthey. The catalyst characterisation has been reported in a previous publication [8]; the Si:Al ratio is 30 and the surface area 371 $m^2 g^{-1}$. The as received catalyst was calcined in air at 500 °C in order to remove any residual template. The reaction of dimethylether was conducted in the Glasgow/ISIS gas manifold and reactor system located in the ISIS Neutron and Muon Experimental Facility (Rutherford Appleton Laboratory) which is described in detail elsewhere [25]. The reactor allows for 10–20 g of samples to be prepared. (Large sample sizes are a prerequisite for INS measurements.) A fixed bed reactor with an internal diameter of 35 mm and length 60 mm was used in all reactions. The reactor is charged with 12 g of calcined catalyst which is then dried under He (150 ml min^{-1}, CK Gas > 99%) at 350 °C. After the drying process is complete, DME (Sigma Aldrich, ≥99.9%) is introduced into the reactor at varying flow rates and times-on-stream (see Table 1). The reactor was kept at 350 °C for the time specified for each reaction. After the reaction was complete, the DME flow and heating was stopped and the sample was left to cool under 150 ml min^{-1} Helium.

2.2. Product analysis

Gaseous products are analysed by in-line mass spectrometry (Hiden Analytical, HPR-20) connected to the exit line of the reactor via a differentially-pumped heated quartz capillary. A catch-pot placed downstream of the catalyst collects liquid products which are analysed by offline GC–MS (Shimadzu QP2010SE, DB-1MS capillary l: 60 m, d: 0.25 mm, t: 0.25 μm) at an initial oven temperature of 40 °C for 2 min, increased at 10 °C min^{-1} to 150 °C held for 3 min.

Table 1
Details of samples prepared.

Sample	Sample Treatment	DME Flow ml/min	He Flow ml/min	Duration hours	WHSV h^{-1}
clean ZSM-5	*ZSM-5 + He*	*–*	*150*	*3*	
DME-1D	*ZSM-5 + DME*	*50*	*106*	*24*	*0.5*
DME-2D	*ZSM-5 + DME*	*80*	*106*	*36*	*0.8*
DME-3D	*ZSM-5 + DME*	*30*	*106*	*72*	*0.3*

2.3. Catalyst analysis

All sample handling was conducted in an argon filled glovebox (MBraun UniLab MB-20-G, $[H_2O] < 1$ ppm, $[O_2] < 1$ ppm). The reacted catalyst was removed from the reactor with most of the sample being transferred into aluminium INS flat cells sealed with indium wire. INS spectra were obtained with the MERLIN and TOSCA instruments located at the ISIS Facility. MERLIN [26] is a direct geometry inelastic spectrometer, and the spectra were acquired by using the A-chopper package at incident energies of 4809 cm^{-1} and 2004 cm^{-1}. MERLIN spectra are integrated over the momentum transfer range of $0 \leq Q \leq 12 Å^{-1}$. MERLIN has only modest resolution across the entire 0 – 4000 cm^{-1} range, but crucially provides access to the C–H and O—H stretch region. TOSCA [27] is an indirect geometry inelastic spectrometer with a spectral range from 0 – 4000 cm^{-1} that is optimal below 2000 cm^{-1}. The advantages of each type of instrument and their complementarity are explored elsewhere [28]. Reference spectra of o-xylene (Sigma Aldrich, 99.9%), durene (Sigma Aldrich, 98.7%) and methanol (Sigma Aldrich, 99.9%) were also recorded by the MERLIN instrument.

The remainder of the reacted samples were kept for *ex situ* analysis using TPO, NMR and nitrogen sorption. TPO experiments were conducted on post-reaction catalyst samples using a Micrometrics Chemisorb 2720 instrument equipped with a thermal conductivity detector. The TPO samples were kept under argon atmosphere for approximately 4 weeks before the TPO measurements were conducted and for each measurement 5 mg of sample was used. Samples were purged with helium (25 ml min^{-1}) before being heated in 5% O_2/He (25 ml min^{-1}) at a rate of 10 °C min^{-1} until 800 °C was reached. The final temperature was maintained for 30 min to ensure the complete combustion of any carbonaceous species.

For NMR analysis, used catalyst samples were loaded in air into 7.5 mm MAS rotors and spectra recorded on a Varian Infinity Plus 400 MHz spectrometer. Sample rotors were spun in dry air at typically 3–4 kHz. ^{13}C spectra were recorded at 100.54 MHz using a variable amplitude cross polarisation pulse sequence and a contact time of 7 ms. Chemical shifts were externally referenced to tetramethylsilane (TMS) via a hexamethylbenzene standard, and typically 60,000 acquisitions averaged with a 5 s pulse delay. ^{27}Al spectra were recorded at 104.2 MHz using a one pulse Bloch decay with a 0.5 μs pulse width ($\pi/20$) and a 5 s pulse delay. All samples were measured with the same number of 500 acquisitions to allow comparison of signal to noise, and chemical shifts externally referenced to a kaolin standard (-2.5 ppm relative to $Al(H_2O)_6^{3+}$). ^{29}Si spectra were recorded at 79.4 MHz using a one pulse Bloch decay with proton decoupling, a $\pi/2$ pulse width of 6 μs and a 5 s pulse delay, typically 1000 acquisitions. ^{29}Si spectra were externally referenced to TMS via a kaolin standard (-91.2 ppm).

Surface area analysis was performed using a Quantachrome Quadrasorb EVO/SI gas adsorption instrument. 0.15 g samples of the material for analysis were added to 9 mm quartz sample tubes and weighed. These were degassed to < 20 mTorr at 473 K using a vacuum degassing rig and mounted on the Quadrasorb instrument. Liquid nitrogen was used as the coolant and N_2 as the adsorbant gas. Gas adsorption and desorption isotherms were collected across a relative pressure (P/P_0) range from 5×10^{-4} – 0.99. Isotherm analysis to generate the sample parameters reported was carried out using the QuadraWin analysis software supplied with the instrument.

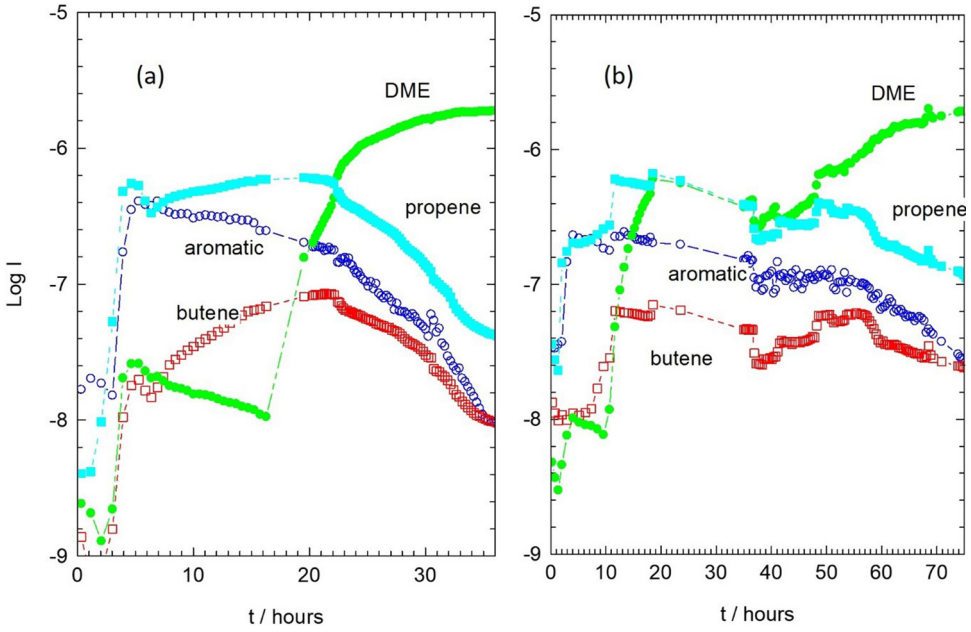

Fig. 1. Mass spectral analysis of evolved gaseous products during DME conversion at 350 °C. (a), 2 day run; (b), 3 day run. DME measured as m/e = 45, propene m/e = 41, butene m/e = 55, aromatics as tropylium ion, m/e = 91.

3. Results and discussion

3.1. Reaction monitoring (Mass Spectrometer and GC–MS)

The mass spectrometric analyses of effluent gases during the two and three day runs are presented in Fig. 1. Both show similar trends. After an initial break-in period of ~ 2 h there is a steady evolution of alkene and methylaromatic products. This continues for 15–20 hours on stream, after which DME conversion begins to fall, as does the yield of alkene and aromatic products. The catalyst still retains some activity and does not become completely deactivated. For the one day run, the DME conversion and yields of products remained approximately constant over the 20 h span of the experiment. Off-line GCMS analysis of the catchpot samples from each run showed similar reaction products in each case: trimethylbenzenes (30–40%) and tetramethylbenzenes (20–30%) being the major products, followed by lesser amounts of xylenes (typically < 15%) and small amounts of methylnaphthalenes and unidentified alkanes.

3.2. TPO analysis

TPO analysis was used to characterise the coke percentage present in the reacted catalyst and to confirm the observations of deactivation from the reaction profiles. TPO of the used catalysts after reaction indicate a weight loss between 200 °C–800 °C indicative of CO and CO_2 generation. Table 2 shows the coke contents of the three used catalysts determined by TPO along with the nitrogen sorption data.

The coke content and surface area/micropore data are broadly similar to values reported in the literature for ZSM-5 catalysts used in methanol conversion. In particular, Bibby et al. reported that complete deactivation of methanol conversion occurred at coke levels between about 14 and 18 wt %, depending on the particular zeolite used. [29] The loss of surface area/micropore volume in the used catalysts is also similar to that reported in [29]. There are nevertheless some differences between the DME-2D and DME-3D catalysts. The DME-2D and DME-3D samples were exposed to dimethylether for different times and at different flow rates (Table 1). The DME-2D catalyst deactivates more quickly than the DME-3D catalyst, which may be due to the higher DME flow rate, and contains a higher level of coke. There is also a significant difference in the TPO profile for the DME-3D catalyst compared with the two exposed to DME for shorter times (Fig. 2). The TPO profiles of DME-1D and DME-2D shown in Fig. 2, are quite symmetrical with a maximum CO/CO_2 desorption at ~ 600 °C. The TPO profile of DME-3D shows a higher maximum temperature of ~ 635 °C. Both types of profile fall into the category of Type II coke assigned by Muller et al to aromatic hydrocarbon species formed in the conversion of methanol to olefins over ZSM-5 at 450 C. [30] The type I coke with a TPO maximum below 400 C and attributed by these authors to oxygenated molecules was not seen in our measurements. Choudhary et al. distinguished

Table 2
Coke content and Nitrogen Sorption Data for Used Catalysts.

Catalyst	Coke content/ wt %	Surface area / $m^2\,g^{-1}$	$V_{micropore}$/ $cm^3\,g^{-1}$
Fresh catalyst	0	387	0.148
DME-1D	8.8	176	0.047
DME-2D	18.7	43.7	0.013
DME-3D	14.6	31.5	0.008

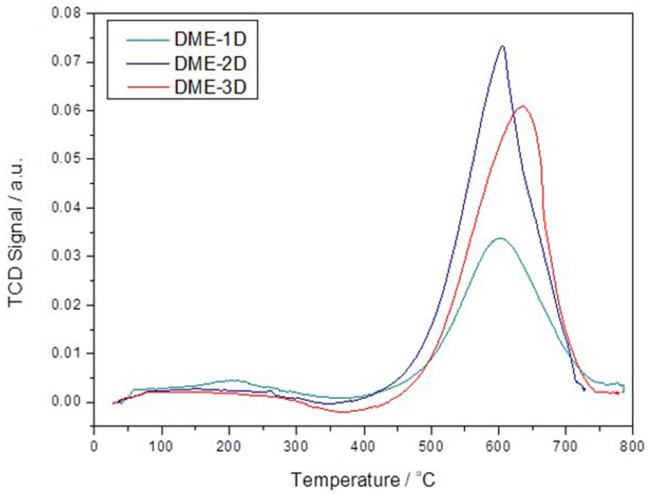

Fig. 2. TPO Profiles of DME-1D, DME-2D and DME-3D.

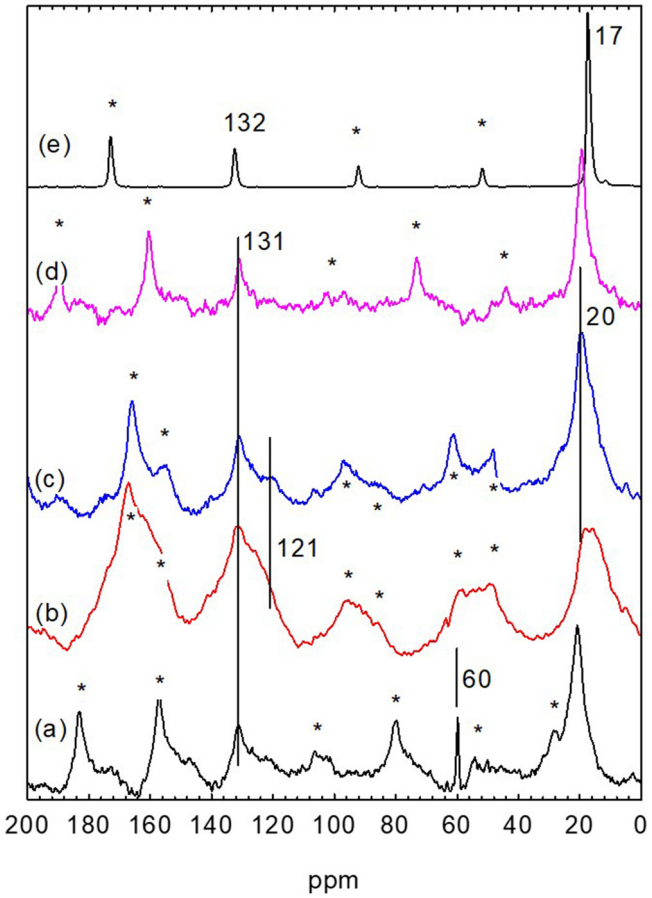

Fig. 3. ^{13}C CPMAS spectra of: (a), DME 1D, 2.6 kHz; (b), DME 2D, 3.5 kHz; (c), DME 3D, 3.5 kHz; (d) Zeolite reacted with methanol at 523 K for 3 days, 3.0 kHz [8], (e) hexamethylbenzene, 4.0 kHz. * denote spinning side bands resulting from the spinning speed indicated.

between "soft" (TPO maximum < 600 C) and "hard" (TPO maximum ~ 650 C) coke formed in the aromatisation of propane over gallosilicate MFI catalysts, and suggested that the "hard" coke is more graphitic in nature with a lower H:C ratio. [31].

3.3. ^{13}C-NMR Analysis

To further probe the molecular identity of coke species present in the used catalysts we undertook ^{13}C CPMAS NMR measurements on the used catalysts. Fig. 3 compares the spectra obtained with that of the same zeolite catalyst used to convert methanol at 350 C for three days (described in reference [8].

There are three regions of interest. Signals around 20 ppm are due to aliphatic carbon, most probably methyl groups. [32] A sharp signal at 60 ppm in the catalyst reacted for only 1 day is due to unreacted (weakly bound) dimethylether [33]. The remaining features are due to aromatic carbons. These give intense spinning side band features separated by the spinning speed employed (between 3 and 4 kHz in the spectra shown here), due to the large chemical shift anisotropy of the aromatic ^{13}C. The spinning side bands are identified by observing their shifts on changing the spinning speed. The unshifted peaks are the isotropic chemical shifts of the species concerned. The spectrum shown in Fig. 3(d) of a catalyst reacted with methanol for three days at 350 C (and still active for hydrocarbon formation [8]) shows a single aromatic carbon signal at ~ 131 ppm with its associated spinning side bands, which resembles but does not match exactly the spectrum of hexamethylbenzene shown in Fig. 3(e). The same signal also dominates the spectrum of the catalyst reacted with dimethylether for 1 day (and still active) shown in Fig. 3(a). The two partially deactivated catalysts (Fig. 3(b) and (c)) show broadening of the 130 ppm signal and the appearance of a definite new component at ~124 ppm. Note that the resolution of this second aromatic component becomes more clear in the spinning side bands. The largest contribution from this component is found in the DME-2D sample which has the highest coke content and the greatest extent of deactivation.

Although there have been extensive ^{13}C NMR studies reported in the literature of the initial stages of methanol conversion over ZSM-5 [7] there is little prior information available on deactivated catalysts. Meinhold and Bibby [34] reported NMR evidence for the presence of methylaromatic species in coked ZSM-5 catalysts. In particular, a signal at ~20 ppm was assigned to methyl groups in tetramethylbenzene isomers, significantly shifted from the 17.2 ppm signal of methyl groups in hexamethylbenzene. This difference is also evident in the spectra shown in Fig. 3. A signal around 130 ppm with strong spinning sidebands was assigned to aromatic carbons, although it was not possible to identify particular species. 20 ppm and 130 ppm signals from coked ZSM-5 have also been reported more recently by Barbera et al. [32], although both show higher and lower field shoulders suggestive of multiple methyl aromatic species.

For the samples analysed here, we can conclude that the DME-1D sample, like the sample exposed to methanol for three days at 350 C, contains mostly tetramethylbenzene species. In the more deactivated samples (DME-2D and DME-3D) there is a growing contribution from other species which may include pentamethylbenzenes and methylated naphthalenes. Particularly in the DME-2D sample there is a much larger ratio of aromatic to aliphatic carbon, although this cannot be quantified without knowing cross-polarisation efficiencies. We note also the cautionary remarks of Meinhold and Bibby [34] that not all of the carbon present in coked catalysts may be NMR visible, due to relaxation effects resulting from the formation of conductive graphitic coke species.

3.4. ^{27}Al and ^{29}Si NMR Analysis

Fig. 4 shows ^{27}Al spectra of the fresh catalyst and the three used DME catalysts. The dominant signal in the fresh catalyst at 51 ppm is due to tetrahedral aluminium in the zeolite framework [35], while the small signal at ~ -3 ppm is attributed to octahedral Al species not in the framework. There is a dramatic decrease in the amount of NMR visible aluminium in the coked zeolites, and the remaining tetrahedral signal is shifted to higher field (by 2–4 ppm). These effects have been seen before in coked ZSM-5 catalysts, and attributed to interaction of coke species with the AlO_4 framework sites, causing broadening of the signal from quadrupolar ^{27}Al beyond detection in a one pulse measurement. [29] Note that the octahedral Al signal is also completely removed. There is no evidence in Fig. 4 for formation of 5 coordinate extra-framework aluminium. However, ^{29} Si NMR spectra in Fig. 5 show that during reaction some loss of lattice AlO_4 aluminium occurs. The major ^{29}Si NMR signal at -113 ppm is due to Q_4 $Si(OSi)_4$ units in the framework, while the shoulder at -107 ppm is due to Q_3 $Si(OSi)_3(OAl)$ units. It is clear that even after 1 day of reaction with DME there has been some framework dealumination, causing a decrease in the -107 ppm signal. It does not appear to decrease further with longer reaction times, although the overall line-width of the ^{29}Si signal is increased as the coke level rises. This framework dealumination is attributed to the steam produced in the initial stages of the reaction, as reported elsewhere. [36].

3.5. Inelastic Neutron Scattering Spectroscopy

Fig. 6 shows INS spectra recorded from the three used catalysts in the low to mid frequency region using the TOSCA spectrometer. The intensities of the spectra have been normalised to account for the differing masses of each sample during the spectral acquisition. Intensity in INS spectra is directly related to the number of inelastic scatterers in

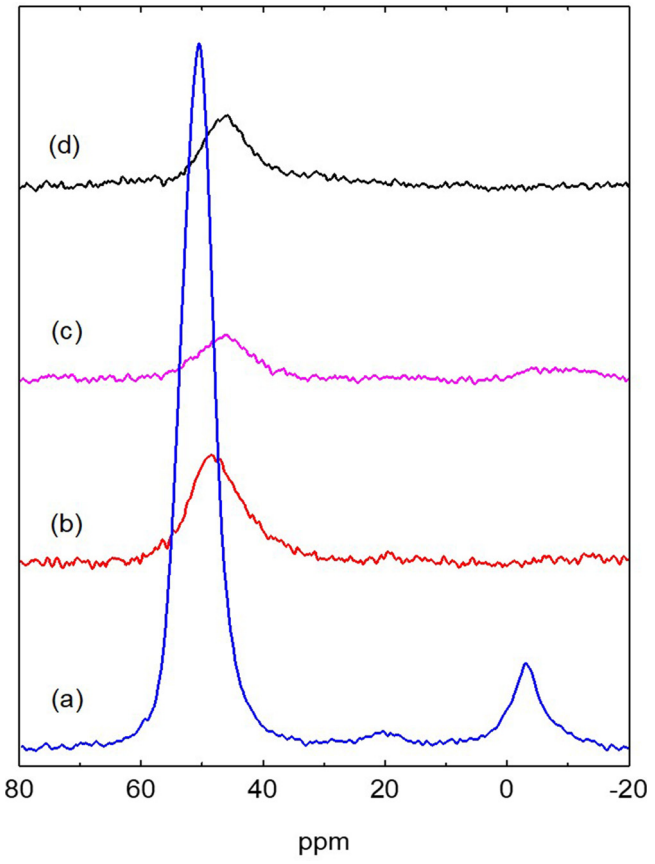

Fig. 4. ^{27}Al NMR spectra of (a) fresh ZSM-5 catalyst; (b) DME-1D sample; (c) DME-2D sample; (d) DME-3D sample. All spectra have been normalised to the same S/N to allow an approximate comparison of intensities.

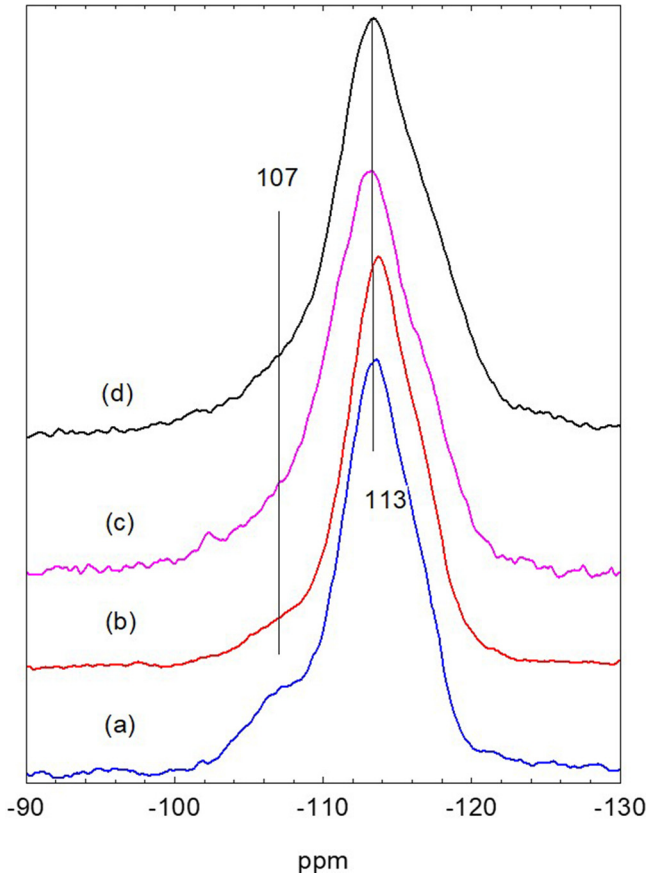

Fig. 5. ^{29} Si NMR spectra of (a) fresh catalyst; (b) DME-1D; (c) DME-2D; (d) DME 3D.

the sample. When comparing the spectra from the three different reacted samples (Fig. 3), we see that the deactivated samples (DME-2D and DME-3D) contain more hydrocarbon content than the still working catalyst (DME-1D). We note that the differences in the spectra from the working catalyst to the deactivated catalyst are minimal, which suggests that the hydrocarbons present during the steady state stage of the catalyst are similar to the hydrocarbons present when the catalyst is in its deactivating phase.

The corresponding high frequency spectra measured with the MERLIN instrument are shown in Fig. 7.

The intensities in the CH stretching region should scale with the coke content determined by TPO analysis if the coke content is solely hydrocarbon. In fact, the DME-2D and DME-3D samples have identical INS spectra, suggesting that the higher coke content of the DME-2D sample may be due to a graphitic component not contributing directly to the INS. This suggestion is also consistent with the additional broadening observed in the ^{13}C NMR spectra for the DME-2D sample.

To try and understand better the INS spectra of the coked catalysts we also recorded INS spectra of durene and o-xylene. Both of these are products detected in MTH steady state and it has been suggested that they may also contribute to deactivation [19,31,37]. Fig. 8 compares the high frequency spectra of these two model compounds with that of the DME-3D sample. The ν(CH) region for durene contains predominantly contributions from sp^3 CH_3 stretching vibrations, since there are 12 sp^3 CH bonds compared with 2 aromatic CH bonds, which vibrate at higher frequency. In o-xylene, the ratio of sp^3 CH bonds to aromatic CH bonds is 6 to 4. Since INS intensities depend directly on the number of hydrogen atoms involved, the profile of the ν(CH) vibrations shifts to higher wavenumber for o-xylene compared with durene. For the DME-3D catalyst, the profile shifts further to higher frequency, suggesting that the ratio of sp^3 CH to aromatic CH is even lower than that in o-xylene. In our previous study of used methanol conversion catalysts we found the sp^3 CH to aromatic CH ratio to be ~ 1:1. In the case of the DME catalysts, the ratio is clearly less than unity.

The spectra of the same three samples measured in the low-medium energy region with the TOSCA instrument are much more complex and are not yet fully assigned. (Fig. 9). There are nevertheless many features in common between the model compounds and the used catalyst, at least in the region above 800 cm^{-1}. For example, the pair of bands at 1370 and 1450 cm^{-1} are due to symmetric and asymmetric CH_3 bending modes, while CH_3 rocking modes and aromatic CH out of plane bending modes occur between 860 and 1050 cm^{-1}. There is arguably a closer alignment between the spectra of the used catalysts and that of o-xylene in this region than with that of durene, which is consistent with the suggestion that the aromatic species in the used catalysts are not highly methylated. The lack of agreement between the spectra of the used catalysts and the model compounds below 800 cm^{-1} is understandable. The model compounds were run as solids at < 30 K, and the low frequency spectra of the solids will contain many librational modes which will not be found in individual molecules trapped in zeolite pores.

Polymethylated aromatics are considered to form in sequential methylation steps which heavily depend on the Brønsted acid sites of the zeolite and the presence of methanol and/or DME [38,39]. One major difference between using DME as reactant rather than methanol is the reduced amount of water formed. As seen in this work, the catalysts deactivate more quickly when DME is the reactant, presumably because regeneration of the Bronsted acid sites needed to catalyse methylation reactions is inhibited at the lower water levels found.

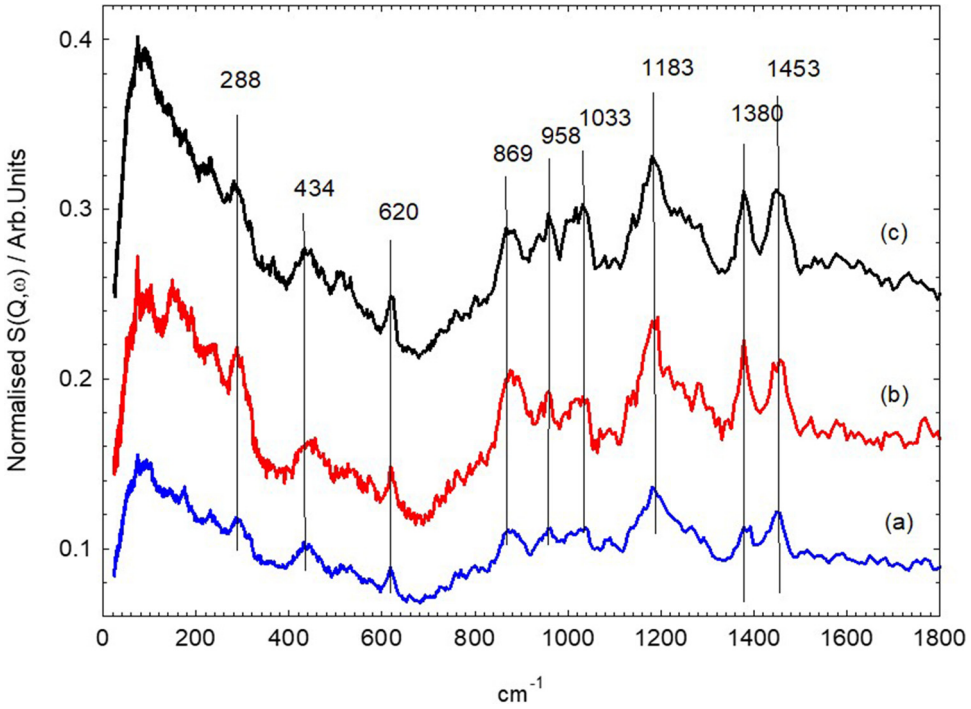

Fig. 6. INS spectra measured with the TOSCA instrument from (a) DME-1D; (b) DME-2D; (c) DME-3D. Spectra have been normalised for the amount of catalyst measured and displaced vertically by a fixed increment to for ease of viewing.

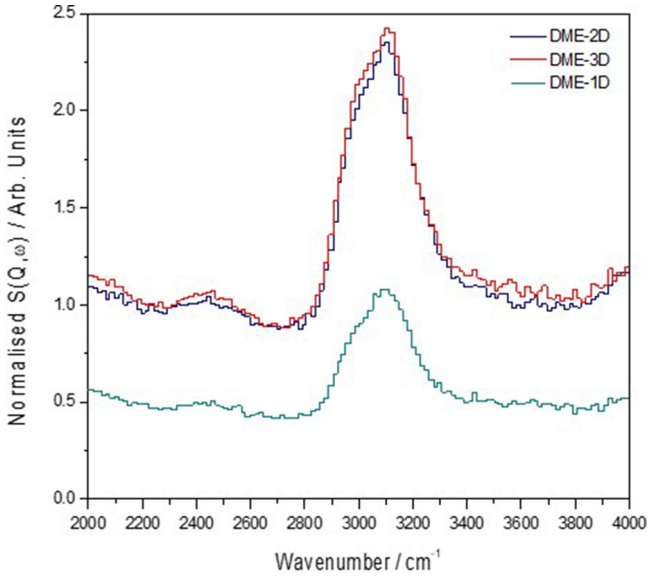

Fig. 7. INS spectra measured with the MERLIN instrument. Spectra have been normalised for the amount of catalyst measured and displaced vertically by a fixed increment for ease of viewing.

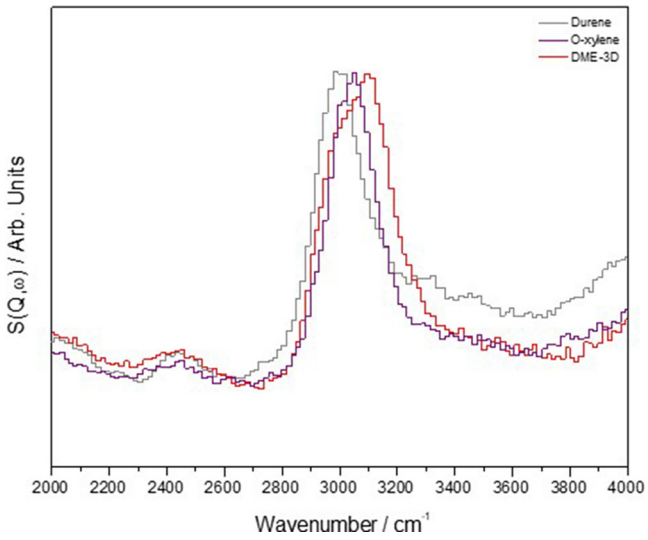

Fig. 8. INS spectra measured with the Merlin instrument in the ν(CH) region of two model compounds and the DME-3D used catalyst.

4. Conclusions

This study has shown that INS can significantly augment the information obtained from other more conventional characterisation techniques for examining the coke deposits in working catalysts for hydrocarbon production from dimethylether. We have found that dimethylether conversion is deactivated more quickly than methanol conversion over the same catalyst at the same temperature, and that the deactivation is enhanced at higher space velocity. In comparison with methanol conversion, the aromatic to aliphatic ratio in the coke deposits is considerably higher; which together with the reduced catalyst lifetime is attributed to the lower levels of water present in DME conversion, reducing the regeneration of acid sites needed for methylation of aromatic species in the zeolite.

The advantages of INS over other vibrational spectroscopies for characterisation of used catalysts are well demonstrated here. The method lacks the spectroscopic resolution of infrared spectroscopy in the CH stretching region, but access to the full vibrational range is a strong feature of the method. More work is needed to assign fully and explain all of the lower frequency bands detected in the coked zeolites, but the ability of INS to interrogate industrial catalyst samples taken directly from a reactor with no sample preparation required should be more widely exploited.

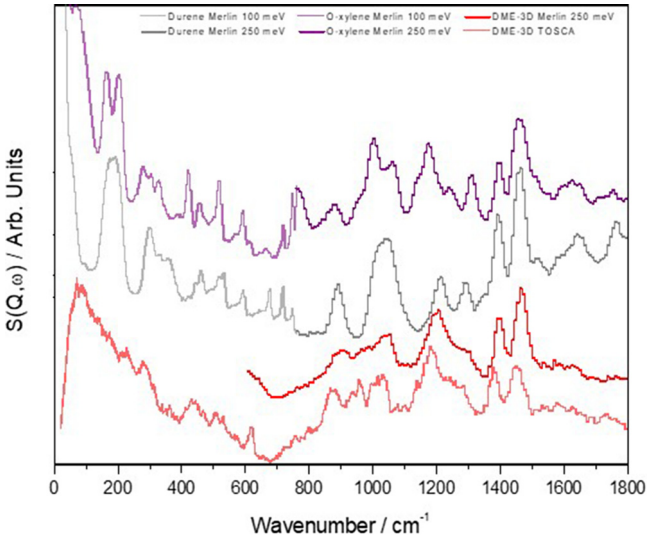

Fig. 9. INS spectra measured with the Merlin and Tosca instruments of o-xylene (top), durene (middle) and the DME-3D used catalyst (bottom). Spectra displaced vertically by a fixed increment for ease of viewing.

Declarations of Interest

None.

Acknowledgements

The UK Catalysis Hub is thanked for resources, support and access to the Research Complex at Harwell which is provided via our membership of the UK Catalysis Hub Consortium and funded by EPSRC (grants EP/K014706/1, EP/K014668/1, EP/K014854/1, EP/K014714/1 and EP/M013219/1). The STFC Rutherford Appleton Laboratory is thanked for access to the neutron beam facilities. Johnson Matthey plc is thanked for studentship support via the EPSRC Industrial CASE scheme (AZ and AH), and the provision of the ZSM5 catalyst plus some characterisation information.

References

[1] S. Teketel, L.F. Lundegaard, W. Skistad, S.M. Chavan, U. Olsbye, K.P. Lillerud, P. Beato, S. Svelle, J. Catal. 327 (2015) 22–32.
[2] B.M. Weckhuysen, J. Yu, Chem. Soc. Rev. 44 (20) (2015) 7022–7024.
[3] S. Teketel, W. Skistad, S. Benard, U. Olsbye, K.P. Lillerud, P. Beato, S. Svelle, ACS Catal. 2 (1) (2012) 26–37.
[4] Z. Wan, W. Wu, G. Li, Kevin, C. Wang, H. Yang, D. Zhang, Appl. Catal. A Gen 523 (2016) 312–320.
[5] Y. Li, C. Zhang, C. Li, Z. Liu, W. Ge, Chem. Eng. J. 320 (2017) 458–467.
[6] M. Westgård Erichsen, S. Svelle, U. Olsbye, M.W. Erichsen, S. Svelle, U. Olsbye, Catal. Today 215 (2013) 216–223.
[7] U. Olsbye, S. Svelle, K.P. Lillerud, Z.H. Wei, Y.Y. Chen, J.F. Li, J.G. Wang, W.B. Fan, Chem. Soc. Rev. 44 (20) (2015) 7155–7176.
[8] Suwardiyanto, R.F. Howe, R.C.A. Catlow, E.K. Gibson, A. Hameed, J. McGregor, P. Collier, S.F. Parker, D. Lennon, Faraday Discuss. 197 (2017) 447.
[9] K. Hemelsoet, J. Van der Mynsbrugge, K. De Wispelaere, M. Waroquier, V. Van Speybroeck, ChemPhysChem 14 (8) (2013) 1526–1545.
[10] D.M. Bibby, R.F. Howe, G.D. Mclellan, Appl. Catal. A Gen. 93 (1992).
[11] P. Perez-Uriarte, A. Ateka, M. Gamero, A.T. Aguayo, J. Bilbao, Ind. Eng. Chem. Res. 55 (23) (2016) 6569–6578.
[12] P. Pérez-Uriarte, M. Gamero, A. Ateka, M. Díaz, A.T. Aguayo, J. Bilbao, Ind. Eng. Chem. Res. 55 (6) (2016) 1513–1521.
[13] E.T.C. Vogt, B.M. Weckhuysen, Chem. Soc. Rev. 44 (20) (2015) 7342–7370.
[14] M. Bjørgen, F. Joensen, K.-P. Lillerud, U. Olsbye, S. Svelle, M. Bjorgen, F. Joensen, K.-P. Lillerud, U. Olsbye, S. Svelle, Catal. Today 142 (1–2) (2009) 90–97.
[15] Keil, F. J. Methanol-to-Hydrocarbons: Process Technology. Microporous Mesoporous Mater. 1999, 29 (1–2), 49–66.
[16] P. Pérez-Uriarte, A. Ateka, A.G. Gayubo, T. Cordero-Lanzac, A.T. Aguayo, J. Bilbao, Chem. Eng. J. 311 (2017) 367–377.
[17] J.S. Martinez-Espin, M. Mortén, T.V.W. Janssens, S. Svelle, P. Beato, U. Olsbye, Catal. Sci. Technol. 7 (13) (2017) 2700–2716.
[18] P. Pérez-Uriarte, A. Ateka, A.T. Aguayo, A.G. Gayubo, J. Bilbao, Chem. Eng. J. 302 (2016) 801–810.
[19] H. Schulz, Catal. Today 154 (3–4) (2010) 183–194.
[20] P. Magnoux, P. Roger, C. Canaff, V. Fouche, N.S. Gnep, M. Guisnet, Stud. Surf. Sci. Catal. 34 (1987).
[21] R.F. Howe, J. McGregor, S.F. Parker, P. Collier, D. Lennon, Catal. Letters 146 (7) (2016) 1242–1248.
[22] A.J. O'Malley, S.F. Parker, A. Chutia, F. Farrow, I.P. Silverwood, V. Garcia-Saki, C.R.A. Catlow, Chem. Commun. 52 (2016) 2897–2900.
[23] A.J. O'Malley, S.F. Parker, C.R.A. Catlow, Chem. Commun. 53 (2017) 12164–12176.
[24] A.J. O'Malley, C.R.A. Catlow, F. Fernandez-Alonso, D.L. Price (Eds.), Experimental Methods in the Physical Sciences, 49 Elsevier Inc., London, 2017, pp. 349–401.
[25] R. Warringham, D. Bellaire, S.F. Parker, J. Taylor, R.A. Ewings, C.M. Goodway, M. Kibble, S.R. Wakefield, M. Jura, M.P. Dudman, et al., J. Phys. Conf. Ser. 554 (2014).
[26] R.I.I. Bewley, R.S.S. Eccleston, K.A.A. McEwen, S.M.M. Hayden, M.T.T. Dove, S.M.M. Bennington, J.R.R. Treadgold, Phys. B Condens. Matter 385 (2006) 1029–1031.
[27] Parker, S. F.; Fernandez-Alonso, F.; Ramirez-Cuesta, A. J.; Tomkinson, J.; Rudic, S.; Pinna, R. S.; Gorini, G.; Fernández Castañon, J. Recent and Future Developments on TOSCA at ISIS. *Journal of Physics: Conference Series*; IOP Publishing, 2014; Vol. 554, p 012003.
[28] S.F. Parker, D. Lennon, P.W. Albers, Appl. Spectrosc. 65 (12) (2011) 1325–1341.
[29] D.M. Bibby, N.B. Milestone, J.E. Patterson, L.P. Aldridge, J. Catal. 97 (2) (1986) 493–502.
[30] S. Muller, Y. Liu, V. Muthusamy, X. Sun, A. van Veen, G.L. Haller, M. Sanchez-Sanchez, J.A. Lercher, J. Catal. 325 (1) (2015) 48–59.
[31] V.R. Choudhary, P. Devadas, S.D. Sansare, M. Gusinet, J. Catal. 166 (2) (1997) 236–243.
[32] K. Barbera, S. Sorensen, S. Bordiga, J. Skibsted, H. Fordsmand, P. Beato, T.V.W. Janssens, Catal. Sci. Technol. 2 (6) (2012) 1196–1206.
[33] W. Wang, Y. Jiang, M. Hunger, Catal. Today 113 (2006) 102–114.
[34] R.H. Meinhold, D.M. Bibby, Zeolites 10 (2) (1990) 121–130.
[35] J. Jiao, W. Wang, B. Sulikowski, J. Weitkamp, M. Hunger, Microporous Mesoporous Mater. 90 (2006) 246–250.
[36] S.K.K. Matam, A.J.J. O'Malley, C.R.A.R.A. Catlow, S. Suwardiyanto, P. Collier, A.P. Hawkins, A. Zachariou, D. Lennon, I. Silverwood, S.F. Parker, et al., Catal. Sci. Technol 8 (2018) 3304–3312.
[37] D. Mores, J. Kornatowski, U. Olsbye, B.M. Weckhuysen, Chem. - A Eur. J. 17 (10) (2011) 2874–2884.
[38] M. Bjørgen, S. Svelle, F. Joensen, J. Nerlov, S. Kolboe, F. Bonino, L. Palumbo, S. Bordiga, U. Olsbye, J. Catal. 249 (2) (2007) 195–207.
[39] S. Ilias, A. Bhan, ACS Catal. 3 (1) (2013) 18–31.